
CausalWrap: Model-Agnostic Causal Constraint Wrappers for Tabular Synthetic Data

Amir Asiaee¹

Zhuohui J. Liang¹

Chao Yan²

¹Department of Biostatistics, Vanderbilt University Medical Center, Nashville, TN, USA

²Department of Biomedical Informatics, Vanderbilt University Medical Center, Nashville, TN, USA

{amir.asiaee@vumc.org, zhuohui.liang.1, chao.yan.1}@vumc.org

Abstract

Tabular synthetic data generators are typically trained to match observational distributions, which can yield high conventional utility (e.g., column correlations, predictive accuracy) yet poor preservation of structural relations relevant to causal analysis and out-of-distribution (OOD) reasoning. When the downstream use of synthetic data involves causal reasoning—estimating treatment effects, evaluating policies, or testing mediation pathways—merely matching the observational distribution is insufficient: structural fidelity and treatment-mechanism preservation become essential. We propose *CausalWrap* (CW), a model-agnostic wrapper that injects *partial causal knowledge* (PCK)—trusted edges, forbidden edges, and qualitative/monotonic constraints—into any pre-trained base generator (GAN, VAE, or diffusion model), without requiring access to its internals. CW learns a lightweight, differentiable *post-hoc correction map* applied to samples from the base generator, optimized with causal penalty terms under an augmented-Lagrangian schedule. We provide theoretical results connecting penalty-based optimization to constraint satisfaction and relating approximate factorization to joint distributional control. We validate CW on simulated structural causal models (SCMs) with known ground-truth interventions, semi-synthetic causal benchmarks (IHDP and an ACIC-style suite), and a real-world ICU cohort (MIMIC-IV) with expert-elicited partial graphs. CW improves causal fidelity across diverse base generators—e.g., reducing average treatment effect (ATE) error by up to 63% on ACIC and lifting ATE agreement from 0.00 to 0.38 on the intensive care unit (ICU) cohort—while largely retaining conventional utility.

1 INTRODUCTION

Synthetic data generation has emerged as a critical tool for enabling data sharing, augmentation, and method benchmarking in high-stakes domains such as healthcare [Walonoski et al., 2018, Choi et al., 2017]. The standard approach trains a deep generative model—generative adversarial network (GAN) [Xu et al., 2019, Park et al., 2018], variational autoencoder (VAE), diffusion model [Kotelnikov et al., 2023], or large language model (LLM)—to approximate the observational joint distribution $P(X)$ and samples new records from the learned model. Conventional evaluation metrics focus on distributional resemblance (marginal statistics, pairwise correlations, Wasserstein distance) or downstream predictive utility (train-on-synthetic, test-on-real, or TSTR) [Yan et al., 2024, Liang et al., 2025].

However, when the downstream task involves causal reasoning—estimating treatment effects, evaluating policies under counterfactual scenarios, or testing mediation pathways—matching the observational distribution may be necessary but insufficient. Causal conclusions rely on the data-generating process preserving conditional independence structure, mechanism modularity, and interventional semantics [Pearl, 2009, Peters et al., 2017]. A synthetic dataset that closely matches observational statistics but distorts the treatment-assignment mechanism or the outcome model can produce misleading treatment effect estimates and flawed policy recommendations [Amad et al., 2025].

Recent work has begun addressing this gap from complementary angles: STEAM [Amad et al., 2025] augments generators with treatment-mechanism-specific losses; TabStruct [Jiang et al., 2025] proposes structural fidelity metrics; DCM [Chao et al., 2023] builds generators directly from causal graphs; and C-DGMs [Stoian et al., 2024] enforce hard domain constraints via differentiable layers (see Section 2 for details).

These approaches are valuable but share a common limitation: they either require a *fully specified* causal graph (e.g., DCM) or address only specific types of constraints (STEAM targets treatment mechanisms; C-DGMs target

domain-knowledge constraints but not causal structure). In practice, domain experts often possess *partial causal knowledge* (PCK): a subset of trusted directed edges (“smoking causes lung cancer”), forbidden edges (“treatment cannot cause age”), temporal orderings, qualitative monotonicity constraints (“increasing drug dose cannot decrease blood pressure”), and directional effect signs. Crucially, practitioners may only have access to samples from an existing off-the-shelf generator—without the ability to modify its architecture or training procedure—and want to improve its causal properties post hoc.

Contributions. This paper introduces CausalWrap, a model-agnostic *post-hoc correction* wrapper that injects PCK into samples from any base tabular generator. Our contributions are:

1. **A flexible causal constraint framework.** We formalize partial causal knowledge as trusted edges, forbidden edges, and qualitative/monotonic constraints, and define differentiable penalty functionals based on kernel independence measures and paired-sample comparisons.
2. **Theoretical results.** We prove penalty-method convergence to constraint-satisfying optima (Theorem 1) and a chain-rule TV bound showing that approximate conditional matching implies joint distributional closeness (Proposition 1).
3. **An augmented-Lagrangian training schedule.** We extend the basic penalty method to an augmented-Lagrangian scheme with dual updates, improving convergence without requiring manual λ -tuning.
4. **Comprehensive experiments.** We evaluate CausalWrap on simulated SCMs (Tier 1), semi-synthetic causal benchmarks (Tier 2: IHDP and an Atlantic Causal Inference Conference (ACIC)-style suite), and a real-world ICU cohort from MIMIC-IV (Tier 3) using a small clinically-plausible constraint set. We wrap three base generators (CTGAN, TabDDPM, TVAE) and include an oracle SCM sampler for Tier 1 as an upper bound when the full causal model is known.

2 RELATED WORK

2.1 TABULAR SYNTHETIC DATA GENERATORS

GAN-based generators include CTGAN [Xu et al., 2019], TableGAN [Park et al., 2018], and CTAB-GAN+ [Zhao et al., 2022]; VAE-based approaches include TVAE [Xu et al., 2019]. Diffusion-based generators such as TabDDPM [Kotelnikov et al., 2023] apply DDPM [Ho et al., 2020] with multinomial and Gaussian diffusion for mixed-type columns, achieving state-of-the-art fidelity. Score-based SDEs [Song et al., 2021] and LLM-based methods (GReaT [Borisov et al., 2023]) provide further alternatives; see Shi et al. [2025] for a survey.

2.2 MEDICAL AND EHR SYNTHETIC DATA

Synthetic electronic health record (EHR) generation is motivated by regulatory barriers to data sharing and privacy risk. MedGAN [Choi et al., 2017] generates multi-label discrete patient records using an autoencoder-GAN architecture. EMR-WGAN [Zhang et al., 2020] improves upon this by incorporating the Wasserstein objective and removing the autoencoder, yielding higher-fidelity EHR simulation. Recent tutorials and reviews emphasize evaluation and reproducibility in health data synthesis [Yan et al., 2024]; Liang et al. [2025] demonstrate clinically grounded synthetic cohort generation for multi-national longitudinal studies.

2.3 CAUSAL MODELS AND CAUSAL GENERATIVE MODELING

SCMs provide a mechanism-based factorization with interventional and counterfactual semantics [Pearl, 2009, Peters et al., 2017]. CausalGAN [Kocaoglu et al., 2018] learns causal implicit generative models structured by a given causal graph, enabling both observational and interventional sampling. DCM [Chao et al., 2023] couples diffusion models with causal graphs for interventional and counterfactual queries. Relational SCM-based synthesis extends to multi-table data [Hoppe et al., 2025]. DeCaFlow [Almodóvar et al., 2025] uses normalizing flows for deconfounding and causal generation.

2.4 TREATMENT-EFFECT-ORIENTED SYNTHETIC DATA AND EVALUATION

STEAM [Amad et al., 2025] proposes desiderata (covariate, treatment-assignment, and outcome preservation) and evaluation metrics tailored to downstream treatment-effect analysis in medicine, augmenting a base generator with mechanism-specific losses. TabStruct [Jiang et al., 2025] emphasizes structural fidelity and introduces “global utility” as an SCM-free proxy metric. Fairness-aware synthetic generation uses causal or counterfactual constraints [Nagesh et al., 2025, Kusner et al., 2017]. Causal-TGAN [Wen et al., 2021] injects a known causal graph into CTGAN’s conditional generation. The “Causality for Tabular Data Synthesis” (CaTS) benchmark [Tu et al., 2024] evaluates tabular generators on causal metrics using high-order structural causal models.

2.5 CONSTRAINED DEEP GENERATIVE MODELS

Stoian et al. [Stoian et al., 2024] show how to transform DGMs into Constrained DGMs (C-DGMs) by adding a differentiable constraint layer that guarantees sample compliance with domain constraints—achieving near-100% compliance compared to $>95\%$ violation rates in unconstrained models. Physics-informed generative models [Yang and Perdikaris, 2018] embed PDE constraints as soft penalties in the generator loss, providing a template for domain-knowledge regularization. Augmented Lagrangian methods for constrained neural network training [Kotary and Fioretto,

2024, Lavado et al., 2023] provide convergence-guaranteed alternatives to fixed-penalty approaches.

2.6 CAUSAL DISCOVERY, INDEPENDENCE TESTING, AND CONSTRAINED OPTIMIZATION

Causal discovery methods—constraint-based (PC/FCI) [Spirtes et al., 2000], score-based (GES) [Chickering, 2002], and continuous (NOTEARS) [Zheng et al., 2018]—can provide partial graphs; CausalWrap uses such knowledge to constrain a generator’s output distribution. Kernel independence measures (Hilbert-Schmidt independence criterion, HSIC [Gretton et al., 2005], distance correlation [Székely et al., 2007], KCIT [Zhang et al., 2011]) serve as differentiable penalties, and penalty/augmented-Lagrangian methods [Bertsekas, 1999] provide the optimization framework. Classifier two-sample tests [Lopez-Paz and Oquab, 2016] offer practical alternatives for distributional comparison.

3 PROBLEM SETUP

3.1 DATA AND BASE GENERATOR

Let $X = (X_1, \dots, X_d) \in \mathcal{X} \subseteq \mathbb{R}^d$ denote a mixed-type tabular record with d columns (continuous or binary; multi-class categorical columns can be one-hot encoded into binary indicators). Let P denote the (unknown) population distribution over \mathcal{X} , and let $\mathcal{D}_n = \{x^{(i)}\}_{i=1}^n \sim P^n$ be the observed dataset.

A *base* synthetic data generator is a (possibly neural) sampling mechanism $G : Z \rightarrow \mathcal{X}$ with latent noise $Z \sim \nu$ (e.g., GAN generator, VAE decoder, or diffusion reverse process). It induces a model distribution Q_{base} on \mathcal{X} . We assume only black-box access to the base model: we can (i) train it on \mathcal{D}_n using its standard procedure (or receive a pretrained model) and (ii) draw samples from Q_{base} . CausalWrap does not require access to the base generator’s internal parameters, training loss, or gradients (see Figure 3 for an overview of the pipeline).

3.2 PARTIAL CAUSAL KNOWLEDGE

We represent available causal knowledge (illustrated in Figure 1) by a tuple $\mathcal{K} = (E^+, E^0, \mathcal{M})$, where:

- $E^+ \subseteq [d] \times [d]$: *trusted* directed edges $i \rightarrow j$ (“ X_i is a direct cause of X_j ”).
- $E^0 \subseteq [d] \times [d]$: *forbidden* edges (“ X_i does not directly cause X_j ”).
- \mathcal{M} : qualitative constraints (monotonicity, sign restrictions). Each $m \in \mathcal{M}$ specifies a 4-tuple (i, j, S, σ) meaning “ X_j is σ -monotone in X_i given X_S ”, with $\sigma \in \{+, -\}$. The conditioning set S is arbitrary and need not correspond to a parent set; the formalism encodes any qualitative monotonic relationship, though in practice the constraints are typically motivated by causal reasoning.

This knowledge may be elicited from domain experts, de-

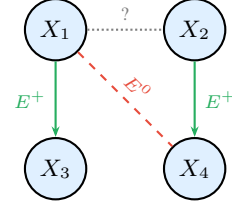


Figure 1: Partial causal knowledge $\mathcal{K} = (E^+, E^0, \mathcal{M})$. **Green solid:** trusted edges (E^+). **Red dashed:** forbidden edges (E^0). **Gray dotted:** unknown status.

rived from temporal structure (e.g., pre-treatment variables precede treatment), or extracted from data via causal discovery algorithms that return partial graphs or equivalence classes [Spirtes et al., 2000, Zheng et al., 2018]. Temporal precedence information can be encoded by adding forbidden edges to E^0 (e.g., forbidding post-treatment variables from directly causing pre-treatment variables).

Example 1 (ICU partial graph). In an ICU cohort, an expert might specify: $E^+ = \{\text{severity} \rightarrow \text{treatment}, \text{treatment} \rightarrow \text{outcome}\}$, $E^0 = \{\text{treatment} \rightarrow \text{age}, \text{treatment} \rightarrow \text{sex}\}$, and $\mathcal{M} = \{\text{severity monotonically increases outcome risk}\}$.

3.3 UTILITY AND CONSTRAINT FUNCTIONALS

Let $\mathcal{U}(P, Q)$ be a distributional loss measuring conventional similarity (e.g., IPM such as Wasserstein W or MMD, or adversarial loss) and let $\Omega_{\mathcal{K}}(Q)$ be a nonnegative functional that quantifies violation of knowledge constraints. We aim to learn a synthetic distribution that trades off conventional resemblance and causal constraint satisfaction:

$$\min_{\phi} \mathcal{U}(P, Q_{\phi}) + \lambda \Omega_{\mathcal{K}}(Q_{\phi}), \quad \lambda > 0. \quad (1)$$

In our setting, $Q_{\phi} := (f_{\phi})_{\#} Q_{\text{base}}$ is obtained by applying a differentiable correction map $f_{\phi} : \mathcal{X} \rightarrow \mathcal{X}$ to samples from a pretrained base generator Q_{base} .

Constraint Functionals. We define $\Omega_{\mathcal{K}}(Q) = \alpha \Omega_{\text{CI}}(Q; E^+, E^0) + \beta \Omega_{\text{mono}}(Q; \mathcal{M})$ as a weighted sum of two types of penalties:

(1) Residualized independence constraints. Let $\text{Pa}^+(j)$ denote the trusted parents of X_j induced by E^+ . We fit simple edge models $\hat{m}_j(X_{\text{Pa}^+(j)})$ on real data (linear regression for continuous targets, logistic regression for binary targets) and define residuals $\tilde{X}_j := X_j - \hat{m}_j(X_{\text{Pa}^+(j)})$ (with $\tilde{X}_j = X_j$ when $\text{Pa}^+(j) = \emptyset$). For each forbidden pair $(a, b) \in E^0$, we penalize dependence between residuals under Q :

$$\Omega_{\text{CI}}(Q) := \sum_{(a,b) \in E^0} w_{a,b} \text{HSIC}(\tilde{X}_a, \tilde{X}_b; Q), \quad (2)$$

where HSIC is computed with a radial basis function (RBF) kernel [Gretton et al., 2005]. This residualization acts as a differentiable proxy for conditional-independence structure implied by the trusted graph (see Figure 2). Although HSIC is symmetric, the residualization step is direction-aware: for

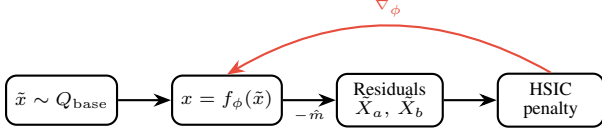


Figure 2: Gradient flow through the CI penalty. **Forward** (black): raw samples pass through f_ϕ ; frozen edge models \hat{m} produce residuals; HSIC on residual pairs gives the penalty. **Backward** (red): gradients flow back through f_ϕ only (edge models are frozen).

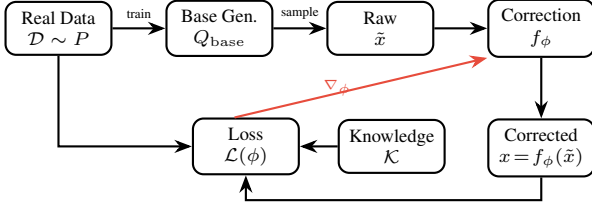


Figure 3: CausalWrap pipeline. A pretrained base generator (frozen) produces raw samples; a correction map f_ϕ produces corrected samples, which—together with real data and partial knowledge \mathcal{K} —feed the loss. **Black**: forward data flow; **red**: gradient (only ϕ is updated).

a forbidden edge $a \rightarrow b$, the residual \tilde{X}_b is computed by regressing out the trusted parents $\text{Pa}^+(b)$, so the penalty structure reflects the directed nature of E^0 . Note that it is a *proxy*, not an exact conditional independence test: if a true parent $X_c \in \text{Pa}(X_b) \setminus \text{Pa}^+(b)$ is missing from the trusted set, its effect remains in the residual \tilde{X}_b . Any correlation of X_a with X_c via another path then inflates $\text{HSIC}(\tilde{X}_a, \tilde{X}_b)$ even though $a \rightarrow b$ is truly absent—a false penalty. In practice this is mitigated when E^+ captures the important parents.

(2) **Monotonic/sign constraints.** For a constraint $(i, j, S, +) \in \mathcal{M}$ (“ X_j nondecreasing in X_i given X_S ”), define a penalty via paired synthetic samples:

$$\Omega_{\text{mono}}(Q) := \sum_{(i,j,S,\sigma) \in \mathcal{M}} \mathbb{E}_{\tilde{x} \sim Q} \left[\max \left(0, -\sigma \cdot \hat{\partial}_{x_i} \mathbb{E}_Q[X_j \mid X_S = \tilde{x}_S, X_i = \tilde{x}_i] \right) \right], \quad (3)$$

where $\hat{\partial}_{x_i}$ is a finite-difference estimate of the conditional effect of X_i on X_j given X_S . Concretely, for each base sample $\tilde{x} \sim Q_{\text{base}}$ we construct a twin \tilde{x}' identical to \tilde{x} except that $\tilde{x}'_i = \tilde{x}_i + \delta$ for a small perturbation $\delta > 0$. Both \tilde{x} and \tilde{x}' are passed through the correction map, yielding $x = f_\phi(\tilde{x})$ and $x' = f_\phi(\tilde{x}')$. A hinge loss penalizes sign violations: $\max(0, -\sigma \cdot (x'_j - x_j))$. The perturbation magnitude δ is a hyperparameter (we use $\delta = 0.5$ in all experiments). Because f_ϕ is differentiable, gradients flow from the hinge loss back through both forward passes to ϕ .

Algorithm 1 CausalWrap (post-hoc correction around a base generator)

Require: data \mathcal{D}_n , pretrained base generator Q_{base} , correction map parameters ϕ , causal knowledge \mathcal{K} , initial λ_0 , growth rate ρ , inner steps T_{inner}

- 1: Initialize dual variables $\mu_c \leftarrow 0$ for each constraint c
- 2: **for** outer iterations $k = 1, 2, \dots, K$ **do**
- 3: **for** inner steps $t = 1, \dots, T_{\text{inner}}$ **do**
- 4: Sample minibatch $\{x^{(i)}\}$ from \mathcal{D}_n and base minibatch $\{\tilde{x}^{(j)}\}$ from Q_{base}
- 5: Apply correction: $x^{(j)} \leftarrow f_\phi(\tilde{x}^{(j)})$
- 6: Compute a utility surrogate $\hat{U}(\mathcal{D}_n, \{x^{(j)}\})$ (e.g., moment matching + identity regularization)
- 7: Compute constraint losses on corrected samples: $\hat{\Omega}_{\text{CI}}, \hat{\Omega}_{\text{mono}}$
- 8: Set ALM loss: $\hat{L} = \hat{U} + \sum_c \mu_c \hat{\Omega}_c + \frac{\lambda}{2} \sum_c \hat{\Omega}_c^2$
- 9: Update ϕ by stochastic gradient step on \hat{L}
- 10: **end for**
- 11: Update duals: $\mu_c \leftarrow \mu_c + \lambda \hat{\Omega}_c(Q_\phi)$ for each c
- 12: Increase penalty: $\lambda \leftarrow \rho \lambda$
- 13: **end for**
- 14: **return** corrected generator $Q_{\hat{\phi}} := (f_{\hat{\phi}})_{\#} Q_{\text{base}}$

4 CAUSALWRAP: A MODEL-AGNOSTIC POST-HOC CORRECTION WRAPPER

4.1 EMPIRICAL OBJECTIVE

Given data \mathcal{D}_n and base synthetic samples $\tilde{x}^{(1:m)} \sim Q_{\text{base}}$, we learn a correction map f_ϕ and optimize an empirical analogue of (1) on the corrected samples $f_\phi(\tilde{x})$:

$$\hat{\phi} \in \arg \min_{\phi} \hat{U}(\mathcal{D}_n, Q_\phi) + \lambda \hat{\Omega}_{\mathcal{K}}(Q_\phi; m), \quad (4)$$

where $Q_\phi := (f_\phi)_{\#} Q_{\text{base}}$.

4.2 AUGMENTED LAGRANGIAN SCHEDULE

A fixed λ requires manual tuning and can lead to under- or over-penalization. We adopt an augmented Lagrangian method (ALM) [Bertsekas, 1999, Lavado et al., 2023] that adaptively adjusts both λ and introduces dual variables μ for each constraint group:

$$\mathcal{L}(\phi, \mu, \lambda) = \hat{U}(\mathcal{D}_n, Q_\phi) + \sum_c \mu_c \hat{\Omega}_c(Q_\phi) + \frac{\lambda}{2} \sum_c \hat{\Omega}_c(Q_\phi)^2,$$

where c indexes individual constraint terms. The full procedure—alternating primal gradient steps, dual variable updates, and penalty increases—is detailed in Algorithm 1; the empirical objective (4) is minimized in each inner loop.

Implementation details—including the correction map architecture, HSIC estimation, monotonicity estimation, binary column handling, and computational overhead—are provided in Appendix B.

5 THEORY

This section formalizes what the CausalWrap wrapper can guarantee. All proofs are deferred to Appendix A.

5.1 PENALTY-METHOD CONVERGENCE

Define the feasible set $\mathcal{F} := \{Q \in \mathcal{Q} : \Omega_{\mathcal{K}}(Q) = 0\}$ and consider the constrained population problem

$$\min_{\phi} \mathcal{U}(P, Q_{\phi}) \quad \text{s.t.} \quad \Omega_{\mathcal{K}}(Q_{\phi}) = 0. \quad (5)$$

Assumption 1 (Basic regularity). (i) *The parameter space Φ is compact.* (ii) $\phi \mapsto \mathcal{U}(P, Q_{\phi})$ and $\phi \mapsto \Omega_{\mathcal{K}}(Q_{\phi})$ are lower semicontinuous. (iii) *There exists at least one feasible parameter $\phi \in \Phi$ with $\Omega_{\mathcal{K}}(Q_{\phi}) = 0$.* (iv) $\inf_{\phi \in \Phi} \mathcal{U}(P, Q_{\phi}) > -\infty$.

Theorem 1 (Penalty convergence). *Under Assumption 1, let $\hat{\phi}_{\lambda}$ be any minimizer of the penalized population objective $\mathcal{U}(P, Q_{\phi}) + \lambda \Omega_{\mathcal{K}}(Q_{\phi})$. As $\lambda \rightarrow \infty$, every limit point ϕ^* of $\{\hat{\phi}_{\lambda}\}$ is feasible and solves the constrained problem (5) (i.e., achieves minimal \mathcal{U} among feasible points).*

Remark 1 (ALM convergence rate). Under standard constraint qualification (linear independence of active constraint gradients at a local minimizer), the augmented Lagrangian method converges at a linear rate in the outer loop, and does not require $\lambda \rightarrow \infty$ —a bounded λ suffices once the dual variables μ track the true Lagrange multipliers [Bertsekas, 1999]. This avoids the ill-conditioning that pure penalty methods suffer from.

5.2 APPROXIMATE FACTORIZATION IMPLIES JOINT CLOSENESS

A key use of causal knowledge is to enforce approximate Markov factorization.

Proposition 1 (Chain-rule total variation (TV) bound for approximate conditionals). *Let P and Q admit factorizations with a common topological order π : $P(x) = \prod_{j=1}^d P_j(x_{\pi(j)} \mid x_{\pi(<j)})$ and $Q(x) = \prod_{j=1}^d Q_j(x_{\pi(j)} \mid x_{\pi(<j)})$. If for all j ,*

$$\mathbb{E}_{X_{\pi(<j)} \sim P} [\text{TV}(P_j(\cdot \mid X_{\pi(<j)}), Q_j(\cdot \mid X_{\pi(<j)}))] \leq \varepsilon_j, \quad (6)$$

then $\text{TV}(P, Q) \leq \sum_{j=1}^d \varepsilon_j$.

Remark 2 (Design rationale and gap). Theorem 1 guarantees that the causal penalties vanish as $\lambda \rightarrow \infty$, and Proposition 1 guarantees that if each conditional is ε_j -close then the joint TV is bounded. However, there is no end-to-end theorem establishing that vanishing HSIC-based penalties imply that Q 's conditionals match P 's—the residualized HSIC is a proxy for conditional independence, not an exact test (see the false-penalty caveat in Section 3). CausalWrap's theory therefore provides a *design rationale* rather than a closed-form guarantee: the penalties are motivated by the chain-rule bound, and empirical results validate that they improve causal fidelity in practice (see Figure 8 in the Supplement).

6 EXPERIMENTS

We evaluate CausalWrap across three tiers of increasing realism. Unless otherwise noted, experiments use 5 random seeds and we report seed-averaged means.

6.1 EXPERIMENTAL SETUP

Base generators. We wrap three base generators spanning GAN/diffusion/VAE families: CTGAN [Xu et al., 2019], TabDDPM [Kotelnikov et al., 2023], and TVAE [Xu et al., 2019]. Each base generator is trained using its standard implementation, and CausalWrap is then fit as a post-hoc correction module on top of base samples.

Oracle comparator (Tier 1 only). For simulated SCMs (Tier 1), we include an oracle comparator that directly samples from the true SCM via ancestral sampling, serving as a full-knowledge reference distribution. Since the average treatment effect (ATE) is estimated using a simple outcome-regression estimator, oracle sampling is not always the lowest ATE error on nonlinear SCMs due to estimator misspecification.

Other causal-aware methods. STEAM [Amad et al., 2025] and C-DGM [Stoian et al., 2024] address different problem settings (treatment-mechanism losses and domain-value constraints, respectively) and are not directly comparable; a systematic cross-regime comparison is left to future work.

Metrics. We evaluate on three axes:

- **Conventional:** MMD (RBF kernel), column-wise Jensen–Shannon divergence (JSD), and TSTR accuracy (train-on-synthetic, test-on-real).
- **Structural:** conditional independence pass rate (CI Pass): the fraction of specified “forbidden” pairs whose absolute residual correlation falls below 0.08 (a correlation-threshold heuristic).
- **Causal:** When ground truth is available (Tiers 1–2), we report ATE absolute error ($|\hat{\tau}_{\text{syn}} - \tau_{\text{true}}|$) and conditional ATE (CATE) precision in estimation of heterogeneous effects (PEHE). When ground truth is unavailable (Tier 3), we report an ATE *agreement* score comparing effect estimates on synthetic vs. real data across an estimator ensemble (OR, IPW, AIPW, TMLE).

6.2 TIER 1: SIMULATED SCMS

Setup. We generate data from three SCM families with known ground-truth interventional distributions:

- **Linear-Gaussian (LG):** $d = 10$ variables, random DAG with expected degree 2, linear mechanisms with additive Gaussian noise.
- **Nonlinear-Additive (NLA):** Same graph structure, nonlinear additive mechanisms using $\tanh(\cdot)$ and a small quadratic term, with additive Gaussian noise.
- **Mixed-Type (MT):** $d = 10$ variables with mixed continuous and binary columns (5 continuous, 5 binary); continuous mechanisms are nonlinear additive and binary mechanisms use a logistic link with Bernoulli noise.

For each SCM we sample $n = 5,000$ training records and generate $m = 5,000$ synthetic records. We set the outcome

Table 1: **Tier 1: CausalWrap improvement (Δ %) in ATE error** across 3 SCM types (5 seeds). **Green** = CW reduces error; **red** = CW increases error. *Gap closed* reports the fraction of the oracle gap closed by CW: $(e_{\text{base}} - e_{\text{CW}})/(e_{\text{base}} - e_{\text{oracle}})$, shown as “-” when $e_{\text{oracle}} \geq e_{\text{base}}$ or when the oracle headroom $(e_{\text{base}} - e_{\text{oracle}})/e_{\text{base}}$ is $< 5\%$ (unstable ratio). **Overall** is the unweighted average across the 3 SCM types. Best partial-knowledge result underlined.

Generator	LG	NLA	MT	Overall
CTGAN	0.832	0.090	0.070	0.331
Δ CW	-9.1%	+11.6%	+23.3%	-4.9%
Gap closed	+29.1%	-	-42.3%	+23.0%
TabDDPM	0.644	0.180	0.042	0.289
Δ CW	-1.7%	+4.6%	-4.8%	-0.6%
Gap closed	+15.4%	-	+19.0%	+5.6%
TVAE	0.766	0.130	0.039	0.312
Δ CW	-6.3%	+0.1%	-2.6%	-5.3%
Gap closed	+25.0%	-	+13.5%	+32.0%
Oracle (true SCM)	0.572	0.177	0.032	0.260

to the sink node $Y = x_d$ and choose treatment T as the earliest ancestor of Y (ensuring a directed causal path). Ground-truth ATE is computed by Monte Carlo ancestral sampling under interventions $\text{do}(T=1)$ and $\text{do}(T=0)$ (100k samples each). Causal knowledge \mathcal{K} is created by revealing 50% of the true edges in E^+ , adding forbidden edges from E^0 (all non-edges involving root nodes), and including 2 monotonicity constraints from \mathcal{M} .

Results. Table 1 summarizes the results (full conventional metrics in Table 2, Appendix D.1). CW consistently improves distributional metrics (MMD/JSD). Its impact on ATE error is modest and mixed: CW improves CTGAN/TVAE on average but is close to neutral for TabDDPM, with SCM-dependent regressions on nonlinear settings. This reflects a trade-off: enforcing causal constraints helps when the base generator violates them but can introduce estimator-facing shifts in harder regimes. On NLA, the linear outcome-regression estimator can be biased even under oracle sampling, muting CW gains. On MT, results are generator-dependent (-4.8% for TabDDPM but $+23.3\%$ for CTGAN), suggesting binary columns pose additional challenges. Tier 1 effects are modest; we next evaluate richer semi-synthetic benchmarks.

6.3 TIER 2: SEMI-SYNTHETIC CAUSAL BENCHMARKS

Setup. We use two standard causal inference benchmarks:

- **IHDP** (Infant Health and Development Program): 747 records, 25 covariates, binary treatment, continuous outcome. We use the widely used semi-synthetic IHDP replications [Hill, 2011] packaged with CEVAE [Louizos et al., 2017] and evaluate 10 replications due to computational cost. Ground-truth potential outcome means (m_0, m_1) are provided, so the individual treat-

ment effect (ITE) is $m_1 - m_0$ and ATE is its mean.

- **ACIC-style suite:** A lightweight semi-synthetic benchmark inspired by ACIC [Dorie et al., 2019] dimensions ($n = 4,800$, $d = 58$, binary treatment, continuous outcome). We evaluate 10 data-generating process (DGP) settings that vary baseline outcome complexity (linear vs. nonlinear) and treatment effect structure (homogeneous vs. heterogeneous), with known ground-truth ITE $\tau(X)$ by construction.

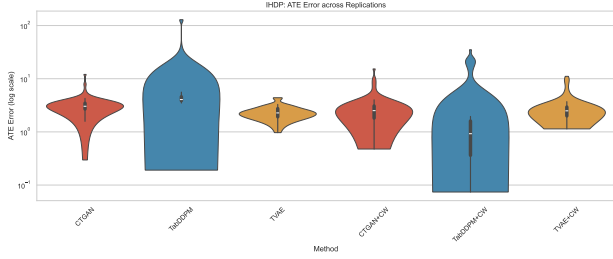
Causal knowledge. For IHDP, we use a small set of illustrative constraints in the benchmark feature space: trusted edges into treatment/outcome ($x_1 \rightarrow \text{treatment}$, $x_2 \rightarrow \text{outcome}$), forbidden edges from treatment to selected covariates (treatment $\rightarrow x_1$, treatment $\rightarrow x_3$), and one monotonic constraint (x_2 positively affects outcome). For the ACIC-style suite, we mark a small subset of covariates as trusted parents of treatment (e.g., $x_1, \dots, x_5 \rightarrow \text{treatment}$) and include a small number of illustrative forbidden edges.

Protocol. For each benchmark setting, we train each generator on the real training data, generate $n_{\text{syn}} = n_{\text{real}}$ synthetic records, then estimate ATE and CATE on the synthetic data using outcome regression. We compare estimated effects to ground-truth. Unless otherwise noted we use 5 random seeds; due to computational cost, ACIC results use 2 seeds and a smaller training budget (50 iterations) for the base generators.

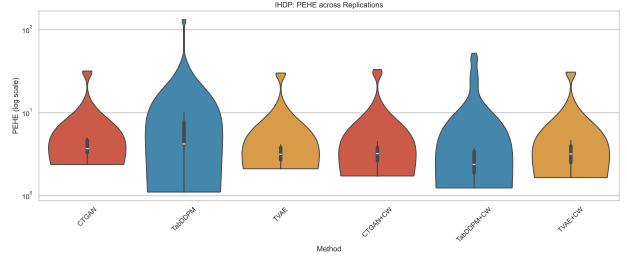
Results. CausalWrap provides its strongest improvements on semi-synthetic benchmarks (Figures 4 and 5). Across IHDP and ACIC settings, the wrapper often reduces ATE error relative to the base generator while largely preserving conventional utility, though gains are not uniform across all bases and settings. For example, on IHDP CW improves CTGAN and TabDDPM mean ATE error (about -7% and -57% , respectively) while increasing TVAE error; on ACIC it substantially improves TVAE (about -63%) and also improves CTGAN and TabDDPM (about -19% and -12%). These patterns are consistent with the intuition behind Proposition 1: when confounding structure is richer, enforcing causal constraints can provide more leverage than on simple simulated SCMs.

6.4 TIER 3: REAL-WORLD ICU COHORT

Setup. We extract an adult ICU cohort from MIMIC-IV [Johnson et al., 2023], retaining the first ICU stay per subject and restricting to adults ($\text{age} \geq 18$). We define a 24-hour baseline window from ICU admission. The resulting cohort ($n = 2,000$) contains demographics (age, sex, race/ethnicity), two binary treatment indicators (any vasopressor administration and mechanical ventilation within the first 24 hours), three baseline laboratory values (lactate, creatinine, white blood cell count (WBC)—first measurement in the window, median-imputed when missing), and outcome (28-day mortality). The cohort has 29% vasopressor-treated patients and 13% mortality.



(a) IHDP: ATE absolute error



(b) IHDP: CATE PEHE

Figure 4: **Tier 2: IHDP benchmark** (10 replications, 5 seeds; log-scale violin plots). CW reduces mean ATE error for CTGAN and TabDDPM but can increase error for TVAE, and may increase tail variance on some replications.

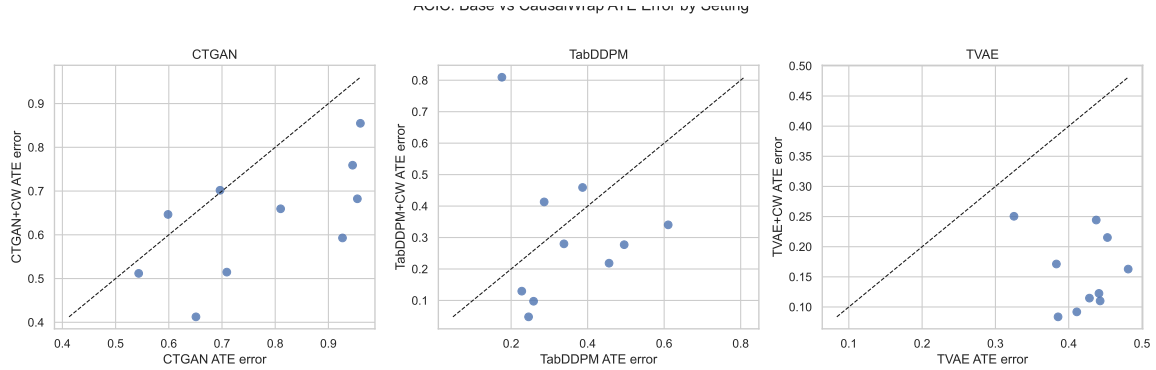


Figure 5: **Tier 2: ACIC-style ATE error across 10 DGP settings** (2 seeds). CW improves all three bases on most settings (largest gains for TVAE), illustrating base-model sensitivity of post-hoc correction.

Causal knowledge. We encode a conservative, clinician-plausible subset of structural knowledge for the 24-hour ICU baseline snapshot (Figure 6). We treat early lactate and creatinine as severity proxies that influence both vasopressor initiation and subsequent mortality risk, and include demographics (age, sex) as stable drivers of treatment propensity. Concretely, E^+ contains trusted edges from baseline covariates to vasopressor treatment and from {age, sex, ventilation, vasopressors, lactate, creatinine} to 28-day mortality, and \mathcal{M} imposes monotonic constraints that increasing lactate and creatinine should not decrease mortality risk. We additionally include temporal forbidden edges E^0 encoding biological and temporal impossibilities: treatment cannot cause pre-treatment demographics, and the outcome cannot retroactively cause baseline-window measurements.

Evaluation. Since ground-truth treatment effects are unknown, we evaluate *agreement* of causal conclusions between real and synthetic data. We compute a reference ATE vector $\{\hat{\tau}_l^{(\text{real})}\}_{l=1}^L$ on the real cohort using an estimator ensemble of $L = 4$ estimators (outcome regression, IPW, AIPW, TMLE) for the vasopressor treatment indicator, compute the analogous vector on synthetic data, and report $1 - \frac{1}{L} \sum_{l=1}^L |\hat{\tau}_l^{(\text{syn})} - \hat{\tau}_l^{(\text{real})}| / (\frac{1}{L} \sum_l |\hat{\tau}_l^{(\text{real})}|)$ (clipped to $[0, 1]$). The estimator ensemble reduces sensitivity to any single misspecified estimator. Reproducing Tier 3 requires cre-

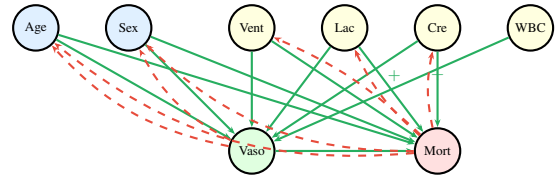


Figure 6: Tier 3 ICU causal knowledge \mathcal{K} . **Green solid:** trusted edges E^+ (demographics, labs, and ventilation cause vasopressor use; treatment and baseline variables cause mortality). **+** on an arrow: monotonic constraint in \mathcal{M} (lactate \uparrow , creatinine \uparrow \Rightarrow mortality risk \uparrow). **Red dashed:** forbidden directions E^0 (temporal/biological impossibilities).

deniated access to MIMIC-IV via PhysioNet [Goldberger et al., 2000]; the cohort extraction and evaluation pipeline will be released with our code upon acceptance.

Results. Figure 7 reports Tier 3 results. CausalWrap lifts ATE agreement for the two generators whose baselines produce zero or near-zero agreement: TabDDPM (0.00 \rightarrow 0.38, the largest absolute gain) and TVAE (0.15 \rightarrow 0.28). For CTGAN, whose uncorrected samples already achieve moderate agreement (0.56), the wrapper’s additional constraints do not improve—and slightly reduce—causal fidelity. On distributional metrics, CW substantially tightens CTGAN’s MMD (−64%) while leaving TSTR essentially unchanged, but for TabDDPM the correction widens the distributional gap (MMD +61%, TSTR −28%), consistent with the Tier 1–2 finding that post-hoc correction faces a steeper fidelity–

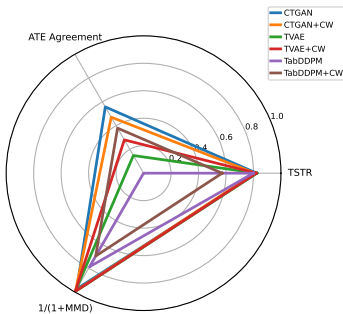


Figure 7: **Tier 3: ICU cohort (MIMIC-IV)**. Radar plot of seed-averaged metrics (TSTR, ATE agreement, and $1/(1 + \text{MMD})$) for each base generator and its CausalWrap variant. All axes are scaled so larger is better.

constraint trade-off when the base generator poorly matches the joint distribution. TVAE shows a non-trivial MMD increase (+40%) alongside its ATE gain. Overall, CW’s benefit is strongest when the base generator clearly violates the causal structure in \mathcal{K} ; when the base already approximately respects the encoded constraints, the optimization budget spent on E^0 and \mathcal{M} penalties yields diminishing returns.

6.5 ABLATION STUDIES

We ablate key design choices using the Linear-Gaussian SCM with TabDDPM as the base generator.

Constraint type ablation. We compare using only CI constraints ($\alpha > 0, \beta = 0$), only monotonicity ($\beta > 0, \alpha = 0$), and both combined (Figure 9a, Supplement). The constraint types contribute differently: monotonicity constraints provide the strongest signal in this setting, while CI constraints can be weaker and may introduce trade-offs when combined.

Knowledge fraction. We vary the fraction of correct edges revealed in E^+ from 0% to 100% (Figure 9b, Supplement). ATE error exhibits a non-monotonic pattern, suggesting that over-constraining the generator can be counterproductive when constraints conflict or over-regularize.

Robustness to wrong edges. We corrupt E^+ by replacing a fraction of edges with incorrect ones (Figure 10a, Appendix D.4). ATE error remains stable under moderate corruption ($\leq 30\%$ wrong edges) without catastrophic degradation.

ALM vs. fixed penalty. The ALM schedule outperforms fixed- λ variants (Figure 10b, Appendix D.4), suggesting that adaptive dual updates reduce sensitivity to penalty tuning.

Forbidden-edge ablation (E^0). Adding temporal forbidden edges to \mathcal{K} improves ATE agreement for TabDDPM but weakens gains for CTGAN and TVAE, likely due to *constraint budget dilution*: HSIC penalties for edges the base generator already approximately satisfies consume optimization capacity without useful gradient signal. Full results are in Table 3 (Supplement).

7 DISCUSSION AND LIMITATIONS

We summarize the main takeaways and acknowledge current limitations.

Theoretical contributions and limitations thereof. CausalWrap provides a principled framework for injecting partial causal knowledge into black-box generators. Theorem 1 guarantees penalty convergence and Proposition 1 relates approximate conditional matching to joint TV control. As discussed in Remark 2, these two results do not compose into a single end-to-end guarantee because residualized HSIC is a proxy for conditional independence, not an exact test. The theory therefore serves as a *design rationale*—motivating the penalty structure—rather than a closed-form bound on $\text{TV}(P, Q)$.

Key empirical findings. Three patterns emerge. (1) *CW’s benefit scales with confounding complexity*: gains are modest on simple simulated SCMs but larger on semi-synthetic benchmarks with richer confounding, consistent with Proposition 1. (2) *Constraint types contribute distinctly*: monotonicity constraints are often the most effective single type; CI constraints can be weaker and may introduce trade-offs when combined, suggesting practitioners should prioritize mechanism-level constraints when available. (3) *Knowledge quality matters non-monotonically*: over-constraining can hurt, wrong-edge corruption shows moderate robustness, and the forbidden-edge ablation (Table 3, Supplement) confirms that redundant E^0 constraints can dilute the optimization budget. CW is best deployed with a conservative subset of high-confidence, *actively violated* constraints.

Limitations. CW can only enforce differentiable penalty functionals; hard combinatorial constraints are not supported. Over-specification can dilute the optimization budget (as shown by the knowledge-fraction and E^0 ablations). The residualized HSIC penalties are proxies for CI with limited statistical power under edge-model misspecification—a likely contributor to weaker CI-only results. As a post-hoc surrogate-utility correction, CW may not preserve higher-order interactions beyond the explicitly enforced constraints. Finally, Tier 3 relies on restricted-access MIMIC-IV data, limiting reproducibility.

Future directions. Natural extensions include longitudinal data (temporal partial orders as forbidden edges), Bayesian graph posterior sampling to weight constraints by posterior probability, and adaptive constraint selection to identify which penalties provide the most gradient signal for a given base generator.

8 CONCLUSION

CausalWrap provides a model-agnostic framework for injecting partial causal knowledge into black-box tabular generators via a lightweight post-hoc correction map. Across simulated SCMs, semi-synthetic benchmarks, and a real-world ICU cohort, CW improves causal fidelity—most strongly when the base generator clearly violates the encoded structure—while largely preserving conventional utility, with the strongest gains when constraints target actively violated causal relationships.

References

- Alejandro Almodóvar, Adrián Javaloy, Juan Parras, Santiago Zazo, and Isabel Valera. DeCaFlow: A deconfounding causal generative model, 2025. arXiv:2503.15114.
- Harry Amad, Zhaozhi Qian, Dennis Frauen, Julianna Piskorz, Stefan Feuerriegel, and Mihaela van der Schaar. Improving the generation and evaluation of synthetic data for downstream medical causal inference, 2025. arXiv:2510.18768.
- Dimitri P. Bertsekas. *Nonlinear Programming*. Athena Scientific, 2nd edition, 1999. ISBN 9781886529052.
- Vadim Borisov, Kathrin Sessler, Tobias Leemann, Martin Pawelczyk, and Gjergji Kasneci. Language models are realistic tabular data generators, 2023. ICLR 2023.
- Patrick Chao, Patrick Blöbaum, Sapan Patel, and Shiva Prasad Kasiviswanathan. Modeling causal mechanisms with diffusion models for interventional and counterfactual queries, 2023. arXiv:2302.00860.
- David Maxwell Chickering. Optimal structure identification with greedy search. *Journal of Machine Learning Research*, 3:507–554, 2002.
- Edward Choi, Siddharth Biswal, Bradley Malin, Jon Duke, Walter F. Stewart, and Jimeng Sun. Generating multi-label discrete patient records using generative adversarial networks. In *Machine Learning for Healthcare (PMLR)*, volume 68, 2017.
- Vincent Dorie, Jennifer Hill, Uri Shalit, Marc Scott, and Dan Cervone. Automated versus do-it-yourself methods for causal inference: Lessons learned from a data analysis competition. *Statistical Science*, 34(1):43–68, 2019.
- Ary L. Goldberger, Luis A. N. Amaral, Leon Glass, Jeffrey M. Hausdorff, Plamen Ch. Ivanov, Roger G. Mark, Joseph E. Mietus, George B. Moody, Chung-Kang Peng, and H. Eugene Stanley. PhysioBank, PhysioToolkit, and PhysioNet: Components of a new research resource for complex physiologic signals. *Circulation*, 101(23):e215–e220, 2000.
- Arthur Gretton, Olivier Bousquet, Alex Smola, and Bernhard Schölkopf. Measuring statistical dependence with Hilbert-Schmidt norms. *Algorithmic Learning Theory*, 2005.
- Jennifer L. Hill. Bayesian nonparametric modeling for causal inference. *Journal of Computational and Graphical Statistics*, 20(1):217–240, 2011.
- Jonathan Ho, Ajay Jain, and Pieter Abbeel. Denoising diffusion probabilistic models. In *NeurIPS*, 2020.
- Frederik Hoppe, Astrid Franz, Lars Kleinemeier, and Udo Göbel. Generating synthetic relational tabular data via structural causal models, 2025. arXiv:2507.03528.
- Xiangjian Jiang, Nikola Simidjievski, and Mateja Jamnik. TabStruct: Measuring structural fidelity of tabular data, 2025. arXiv:2509.11950.
- Alistair E. W. Johnson, Lucas Bulgarelli, Lu Shen, Alvin Gayles, Ayad Shammout, Steven Horng, Tom J. Pollard, Sicheng Hao, Benjamin Moody, Brian Gow, Liwei H. Lehman, Leo A. Celi, and Roger G. Mark. MIMIC-IV, a freely accessible electronic health record dataset. *Scientific Data*, 10(1):1, 2023. doi: 10.1038/s41597-022-01899-x.
- Murat Kocaoglu, Christopher Snyder, Alex Dimakis, and Sriram Vishwanath. CausalGAN: Learning causal implicit generative models with adversarial training. In *ICLR*, 2018.
- James Kotary and Ferdinando Fioretto. Learning constrained optimization with deep augmented lagrangian methods, 2024. arXiv:2403.03454.
- Akim Kotelnikov, Dmitry Baranchuk, Ivan Rubachev, and Artem Babenko. TabDDPM: Modelling tabular data with diffusion models. In *ICML*, 2023.
- Matt J. Kusner, Joshua Loftus, Chris Russell, and Ricardo Silva. Counterfactual fairness. In *NeurIPS*, 2017.
- Diogo Lavado, Cláudia Soares, and Alessandra Micheletti. Achieving constraints in neural networks: A stochastic augmented lagrangian approach, 2023. arXiv:2310.16647.
- Zhuohui J Liang, Zhuohang Li, Nicholas J Jackson, Yanink Caro-Vega, Ronaldo I Moreira, Fabio Paredes, Jordany Bernadin, Diana Varela, Carina Cesar, Alessandro Blasimme, et al. Generating synthetic multi-national longitudinal cohorts for clinically grounded HIV research. *medRxiv*, 2025. Preprint.
- David Lopez-Paz and Maxime Oquab. Revisiting classifier two-sample tests. *arXiv preprint arXiv:1610.06545*, 2016.
- Christos Louizos, Uri Shalit, Joris M. Mooij, David Sontag, Richard Zemel, and Max Welling. Causal effect inference with deep latent-variable models. In *NeurIPS*, 2017.
- Nitish Nagesh, Salar Shakibhamedan, Mahdi Bagheri, Ziyu Wang, Nima TaheriNejad, Axel Jantsch, and Amir M. Rahmani. Fairtabgen: High-fidelity and fair synthetic health data generation from limited samples, 2025.
- Noseong Park, Mohammadreza Mohammadi, Kshitij Gorde, Sushil Jajodia, Hongkyu Park, and Youngmin Kim. Data synthesis based on generative adversarial networks. In *VLDB*, volume 11, pages 1071–1083, 2018.

- Judea Pearl. *Causality: Models, Reasoning, and Inference*. Cambridge University Press, 2nd edition, 2009. doi: 10.1017/CBO9780511803161.
- Jonas Peters, Dominik Janzing, and Bernhard Schölkopf. *Elements of Causal Inference: Foundations and Learning Algorithms*. MIT Press, 2017. ISBN 9780262344296.
- Ruxue Shi, Yili Wang, Mengnan Du, Xu Shen, Yi Chang, and Xin Wang. A comprehensive survey of synthetic tabular data generation, 2025.
- Yang Song, Jascha Sohl-Dickstein, Diederik P. Kingma, Abhishek Kumar, Stefano Ermon, and Ben Poole. Score-based generative modeling through stochastic differential equations. In *ICLR*, 2021.
- Peter Spirtes, Clark Glymour, and Richard Scheines. *Causation, Prediction, and Search*. MIT Press, 2nd edition, 2000.
- Mihaela C. Stoian, Salijona Dyrnishi, Maxime Cordy, Thomas Lukasiewicz, and Eleonora Giunchiglia. How realistic is your synthetic data? constraining deep generative models for tabular data. In *ICLR*, 2024.
- Gábor J. Székely, Maria L. Rizzo, and Nail K. Bakirov. Measuring and testing dependence by correlation of distances. *The Annals of Statistics*, 35(6):2769–2794, 2007.
- Ruibo Tu, Zineb Senane, Lele Cao, Cheng Zhang, Hedvig Kjellström, and Gustav Eje Henter. Causality for tabular data synthesis: A high-order structure causal benchmark framework, 2024.
- Jason Walonoski, Mark Kramer, Josh Nichols, Andrew Quina, Christopher Moesel, Daniel Hall, Colin Duffett, Keith Dube, Thomas Gallagher, and Scott McLachlan. Synthea: An approach, method, and software mechanism for generating synthetic patients and the synthetic electronic health care record. *Journal of the American Medical Informatics Association*, 25(3):230–238, 2018.
- Bingyang Wen, Luis Oliveros Colon, K. P. Subbalakshmi, and R. Chandramouli. Causal-tgan: Generating tabular data using causal generative adversarial networks, 2021.
- Lei Xu, Maria Skoularidou, Alfredo Cuesta-Infante, and Kalyan Veeramachaneni. Modeling tabular data using conditional GAN, 2019. *NeurIPS* 2019.
- Chao Yan, Ziqi Zhang, Steve Nyemba, and Zhuohang Li. Generating synthetic electronic health record data using generative adversarial networks: Tutorial. *JMIR AI*, 3:e52615, 2024. doi: 10.2196/52615.
- Yibo Yang and Paris Perdikaris. Physics-informed deep generative models, 2018.
- Kun Zhang, Jonas Peters, Dominik Janzing, and Bernhard Schölkopf. Kernel-based conditional independence test and application in causal discovery. In *UAI*, pages 804–813, 2011.
- Ziqi Zhang, Chao Yan, Diego A. Mesa, Jimeng Sun, and Bradley A. Malin. Ensuring electronic medical record simulation through better training, modeling, and evaluation. *Journal of the American Medical Informatics Association*, 27(1):99–108, 2020. doi: 10.1093/jamia/ocz161.
- Zilong Zhao, Aditya Kunar, Robert Birke, and Lydia Y. Chen. CTAB-GAN+: Enhancing tabular data synthesis, 2022.
- Xun Zheng, Bryon Aragam, Pradeep Ravikumar, and Eric P. Xing. DAGs with NO TEARS: Continuous optimization for structure learning. In *NeurIPS*, 2018.

CausalWrap: Model-Agnostic Causal Constraint Wrappers for Tabular Synthetic Data (Supplementary Material)

Amir Asiaee¹

Zhuohui J. Liang¹

Chao Yan²

¹Department of Biostatistics, Vanderbilt University Medical Center, Nashville, TN, USA

²Department of Biomedical Informatics, Vanderbilt University Medical Center, Nashville, TN, USA

{amir.asiaee@vumc.org, zhuohui.liang.1, chao.yan.1}@vumc.org

A PROOFS

Proof of Theorem 1. Let ϕ_f be a feasible parameter. For any $\lambda > 0$,

$$\mathcal{U}(P, Q_{\hat{\phi}_\lambda}) + \lambda \Omega_{\mathcal{K}}(Q_{\hat{\phi}_\lambda}) \leq \mathcal{U}(P, Q_{\phi_f}) + \lambda \Omega_{\mathcal{K}}(Q_{\phi_f}) = \mathcal{U}(P, Q_{\phi_f}).$$

Since $\mathcal{U}(P, Q_{\hat{\phi}_\lambda}) \geq \inf_{\phi} \mathcal{U}(P, Q_{\phi}) > -\infty$, we obtain $\lambda \Omega_{\mathcal{K}}(Q_{\hat{\phi}_\lambda}) \leq \mathcal{U}(P, Q_{\phi_f}) - \inf_{\phi \in \Phi} \mathcal{U}(P, Q_{\phi}) =: B < \infty$, so $\Omega_{\mathcal{K}}(Q_{\hat{\phi}_\lambda}) \leq B/\lambda \rightarrow 0$ as $\lambda \rightarrow \infty$.

By compactness of Φ , take a convergent subsequence $\hat{\phi}_{\lambda_k} \rightarrow \phi^*$. Lower semicontinuity gives $\Omega_{\mathcal{K}}(Q_{\phi^*}) \leq \liminf_k \Omega_{\mathcal{K}}(Q_{\hat{\phi}_{\lambda_k}}) = 0$, so ϕ^* is feasible.

To show optimality among feasible points, fix any feasible ϕ . From optimality of $\hat{\phi}_\lambda$, $\mathcal{U}(P, Q_{\hat{\phi}_\lambda}) \leq \mathcal{U}(P, Q_{\phi}) + \lambda \Omega_{\mathcal{K}}(Q_{\hat{\phi}_\lambda}) \leq \mathcal{U}(P, Q_{\phi})$. Taking \liminf along the subsequence and using lower semicontinuity yields $\mathcal{U}(P, Q_{\phi^*}) \leq \mathcal{U}(P, Q_{\phi})$ for all feasible ϕ , proving ϕ^* solves (5). \square

Proof of Proposition 1. We construct a coupling between P and Q via sequential sampling. Define intermediate distributions R_k for $k = 0, \dots, d$ where $R_0 = P$, $R_d = Q$, and R_k uses P 's conditionals for variables $\pi(1), \dots, \pi(d-k)$ and Q 's conditionals for $\pi(d-k+1), \dots, \pi(d)$.

For each consecutive pair (R_{k-1}, R_k) , these differ only in the conditional for variable $\pi(d-k+1)$. Construct a maximal coupling at step $\pi(d-k+1)$: conditional on the history $X_{\pi(<d-k+1)}$ (which is identically distributed under both R_{k-1} and R_k when conditioned on identical past draws), the probability of a mismatch at this step equals $\text{TV}(P_{\pi(d-k+1)}(\cdot | X_{\pi(<d-k+1)}) | Q_{\pi(d-k+1)}(\cdot | X_{\pi(<d-k+1)})$.

Taking expectations over the history and summing over all d steps: $\text{TV}(P, Q) \leq \text{TV}(R_0, R_1) + \dots + \text{TV}(R_{d-1}, R_d) \leq \sum_{j=1}^d \varepsilon_j$. This uses the triangle inequality for TV and the fact that each intermediate TV is bounded by ε_j via the conditional coupling. \square

B IMPLEMENTATION DETAILS

Correction map and utility surrogate. We implement f_ϕ as a small residual MLP initialized near the identity map. We use a lightweight surrogate utility consisting of moment matching (means and covariances between corrected synthetic and real minibatches) plus an identity regularizer $\|f_\phi(\tilde{x}) - \tilde{x}\|_2^2$ to prevent over-correction; this regularizer is set stronger for TabDDPM than for CTGAN/TVAE in our experiments.

Dependence estimation. We use the biased HSIC estimator with a Gaussian RBF kernel whose bandwidth is set by the median heuristic [Gretton et al., 2005]. In our implementation, we (i) fit edge models \hat{m}_j on real data using trusted parents E^+ , (ii) compute residuals \tilde{X}_j on corrected samples, and (iii) apply HSIC to residual pairs specified by E^0 (subsampling pairs for efficiency).

Monotonicity estimation. We estimate monotonicity using paired synthetic samples: we perturb a specified feature by a small δ and apply a hinge penalty to sign violations in the corresponding output change.

Binary columns. For columns detected as binary $\{0, 1\}$, we clamp values to $[0, 1]$ when computing constraint penalties during training. At sampling time, we interpret corrected values as Bernoulli probabilities (with a simple marginal mean-shift calibration) and sample binary values; if a column is already binary and close to the target marginal, we leave it unchanged to avoid injecting additional Monte Carlo noise.

Computational overhead. The constraint penalties add $O(m \cdot |\mathcal{C}| \cdot d_S)$ computation per minibatch for CI constraints (where d_S is the maximum conditioning set size) and $O(m \cdot |\mathcal{M}|)$ for monotonicity. In our settings, the additional overhead is typically modest relative to base training.

Hyperparameters. Unless otherwise noted, we use the following ALM schedule across all experiments: initial penalty $\lambda_0 = 1.0$, growth rate $\rho = 1.5$, Adam optimizer with learning rate 5×10^{-2} . The number of outer iterations is $K_{\text{outer}} = 20$ for Tier 1 and ablations, $K_{\text{outer}} = 10$ for Tiers 2–3. Inner steps per outer iteration match the base generator’s training budget (typically 100–500 steps depending on the generator and dataset size). Monotonicity perturbation magnitude is $\delta = 0.5$ throughout.

C THEORY CONNECTION DIAGRAM

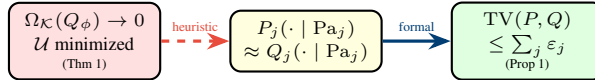


Figure 8: Connecting the theoretical guarantees. Theorem 1 ensures penalties vanish; Proposition 1 converts conditional closeness to joint TV control. The intermediate step (dashed red) is a design motivation: residualized HSIC penalties are a proxy for conditional matching, not a formal equivalence.

D ADDITIONAL EXPERIMENTAL RESULTS

D.1 TIER 1: FULL LG CONVENTIONAL METRICS

Table 2: **Tier 1: CausalWrap on the LG SCM** ($d = 10$, $n = 5,000$, 5 seeds). Each pair shows base \rightarrow +CW. $\Delta\%$ row: **green** = improvement, **red** = degradation. Underline marks the largest ATE error reduction among wrapped bases.

Generator	Conventional			Causal	
	MMD↓	JSD↓	TSTR↑	ATE err↓	CI Pass↑
CTGAN	0.023	0.052	0.744	0.832	0.669
Δ CW	-72.7%	-31.7%	+1.0%	-9.1%	+4.7%
TabDDPM	0.011	0.020	0.763	0.644	0.486
Δ CW	-39.2%	-7.6%	+0.3%	-1.7%	+34.1%
TVAE	0.011	0.056	0.761	0.766	0.916
Δ CW	-24.5%	-36.4%	-0.8%	-6.3%	-13.3%
Oracle (true SCM)	0.003	0.007	0.769	0.572	0.947

D.2 FORBIDDEN-EDGE ABLATION

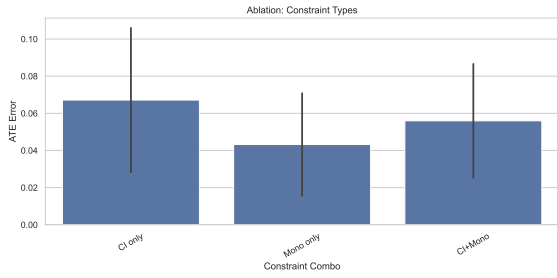
Table 3 compares CausalWrap on the ICU cohort under two knowledge configurations: $E^0 = \emptyset$ (only trusted edges and monotonicity) versus the full \mathcal{K} with temporal forbidden edges. Adding E^0 improves TabDDPM’s ATE agreement gain (+0.38 vs. +0.24) but weakens the gains for CTGAN (which flips from +0.19 to -0.09) and TVAE (+0.31 \rightarrow +0.13). The likely mechanism is *constraint budget dilution*: enforcing edge removal on a frozen model requires more correction to the base residual than correcting ATE bias, and HSIC penalties for forbidden edges that the base generator already approximately satisfies consume optimization capacity without providing useful gradient signal, leaving less room for the beneficial monotonicity and moment-matching terms.

Table 3: **Forbidden-edge ablation** on the ICU cohort (5 seeds). Δ CW reports the change from base to +CW within each knowledge configuration. $E^0 = \emptyset$: trusted edges and monotonicity only. Full \mathcal{K} : adds 7 temporal forbidden edges.

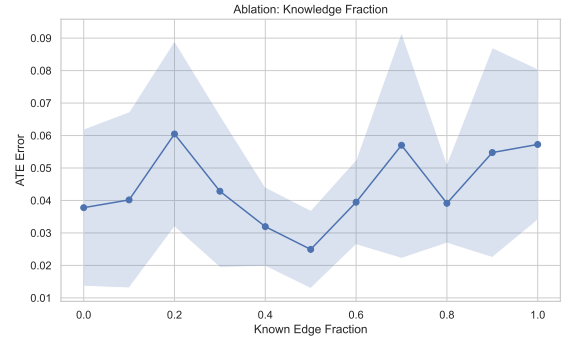
Base	$E^0 = \emptyset$			Full \mathcal{K} (with E^0)		
	Δ MMD	Δ TSTR	Δ ATE	Δ MMD	Δ TSTR	Δ ATE
CTGAN	-69%	+0.1%	+19	-64%	-1.5%	-.09
TabDDPM	+72%	-17%	+24	+61%	-28%	+38
TVAE	-6%	-0.4%	+31	+40%	-0.6%	+13

D.3 CONSTRAINT-TYPE AND KNOWLEDGE-FRACTION ABLATIONS

D.4 ADDITIONAL ABLATION STUDIES

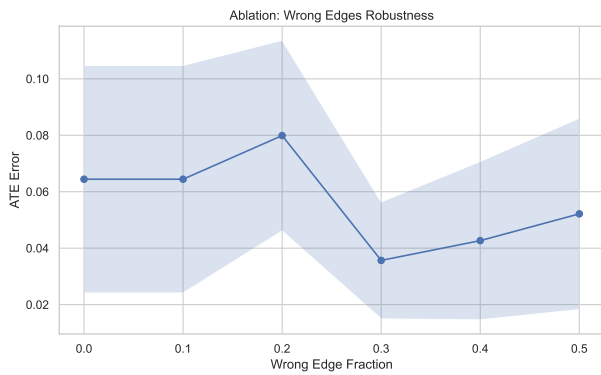


(a) Constraint type ablation

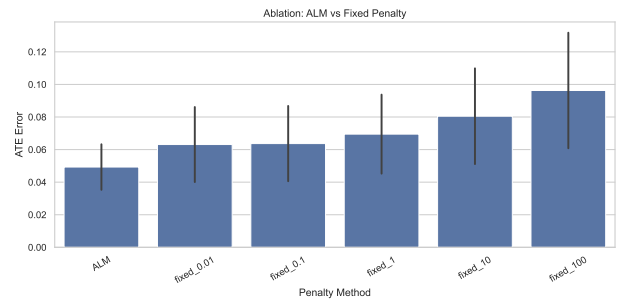


(b) Knowledge fraction

Figure 9: **Ablation studies** on the Linear-Gaussian SCM with TabDDPM base.



(a) Robustness to wrong edges



(b) ALM vs. fixed λ

Figure 10: **Additional ablation studies** on the Linear-Gaussian SCM with TabDDPM base.